DOI: 10.1021/cg901227h

CRYSTAL GROWTH & DESIGN Article

2010, Vol. 10 895–902

Construction of Metal−Organic Frameworks with 1D Chain, 2D Grid, and 3D Porous Framework Based on a Flexible Imidazole Ligand and Rigid Benzenedicarboxylates

Haiyan He,[†] David Collins,[‡] Fangna Dai,[†] Xiaoliang Zhao,[†] Guoqing Zhang,[†] Huiqing Ma,[†] and Daofeng Sun*,[†]

[†]*Key Lab for Colloid and Interface Chemistry of Education Ministry, Department of Chemistry, Shandong University, Jinan 250100, P. R. China, and* [‡]*Department of Chemistry, SUNY Cortland, P.O. Box 2000, Cortland, New York 13045*

Received October 6, 2009; Revised Manuscript Received November 2, 2009

ABSTRACT: Using ligands BITMB and IPA or TMIPA (BITMB = 1,3-bis(imidazol-1-ylmethyl)-2,4,6-trimethylbenzene, IPA = isophthalic acid, TMIPA = 2,4,6-trimethylisophthalic acid), in which the BITMB can adopt *syn* or *anti* conformations, three metal−organic frameworks (MOFs) have been synthesized. These MOFs contain a variety of structures: a one-dimensional (1D) chain (**1**), two-dimensional (2D) interpenetrating layer (**2**), and three-dimensional (3D) porous framework (**3**). In MOFs **1** and **2**, the BITMB ligand adopts a *syn* conformation, connecting metal ions to form a macrometallocycle or chain as the subunit, which are further connected by the rigid carboxylate ligands to generate the final 1D chain or 2D interpenetrating layer. The BITMB ligand in **3** adopts an *anti* conformation, which connects metal ions to form a 1D zigzag chain as the subunit. The 1D chain subunits are further connected by the carboxylate ligand to form the 3D porous framework. The conformation of the BITMB and thus the dimensionality of the MOF can be controlled by the presence or lack of water solvent in the reaction system. Photoluminescence measurements of **2** and **3** in the solid state at room temperature show that both coordination networks exhibit similar, strong luminescence, which can be assigned to an intraligand $\pi\rightarrow\pi^*$ transition.

Introduction

The rational assembly of metal−organic frameworks (MOFs) from organic ligands and metal ions is currently of significant interest due to their interesting topologies and potential applications in nonlinear optics, magnetism, molecular recognition, gas adsorption, etc.[1−3] With the development of supramolecular chemistry and crystal engineering of MOFs, it is possible to design and construct novel MOFs with desired topologies and rationally predict the final structures of the product.[4] However, this predictive ability is mainly limited to MOFs containing rigid organic ligands and rigid SBUs. In contrast to rigid ligands with single conformations, flexible ligands may adopt several kinds of conformation when they coordinate to metal ions, complicating the prediction of final products.[5] Hence, it is still a significant challenge to assemble desired MOFs with interesting properties using flexible organic ligands.

On the other hand, the use of flexible ligands in the construction of MOFs may generate novel complexes with interesting topologies and attractive properties, as flexible ligands have variable coordination modes,[6] and can adopt a variety of conformations according to the restrictions imposed by the coordination geometry of the metal ion and the final three-dimensional (3D) packing. In the past decades, many efforts have been devoted to rational construction of MOFs based on flexible organic ligands.[7] It is generally understood that the assembly of coordination polymers are mainly influenced by the shape and connectivity of the ligand, the coordination geometry of the metal ion, the presence of solvents, and the reaction conditions.[8] However, for the construction of MOFs with a flexible ligand, the ligand conformation would be expected to have a significant effect on the structure of the final product. For example, Sun and co-workers have designed and synthesized a series of metal−organic supramolecules based on a series of flexible bidentate imidazole-containing organic ligands, in which the different conformations of the flexible ligands can result in the formation of different topologies.[9]

One of the most effective strategies to assemble MOFs is to apply mixed multifunctional organic ligands to connect metal ions.[10] The mixed organic ligands may play different roles in the formation of the final structure of the product. In our previous work, we primarily focused on the design and synthesis of functional MOFs based on mixed rigid ligands such as 4,4′-bipyridine and an aromatic acid.[11] Inspired by the above work, we have included a flexible ligand with the carboxylate system to assemble functional MOFs. It is evident that a flexible diimidazole ligand may possess two possible conformations: *syn*- and *anti*-conformation, which can connect the metal ions to generate macrometallocycle or zigzag chain subunits based on the different conformations of the ligand.[12] The connection of these subunits by the secondary rigid carboxylate ligand will result in the formation of functional MOFs of higher dimensionality.

When using a flexible ligand, control of the conformation, and thus control of the dimensionality of the final product, becomes a major challenge. Although several examples of conformational control of such ligand have been reported,[13] control of the dimensionality of the final MOF product via conformational control is still unexplored. Herein, we report three MOFs, Ni(BITMB)(TMIPA)·$2H_2O$ (**1**), which forms a one-dimensional (1D) chain, Zn(BITMB)(IPA)·H_2O (**2**), which forms a two-dimensional (2D) interpenetrating layer,

*Corresponding author. E-mail: dfsun@sdu.edu.cn.

Published on Web 11/19/2009

and $Zn_2(BITMB)_2(HIPA)_2(IPA)\cdot H_2O$ (**3**), which forms a three-dimensional (3D) porous framework (BITMB = 1,3-bis-(imidazol-1-ylmethyl)-2,4,6-trimethylbenzene, H_2IPA = isophthalic acid, H_2TMIPA = 2,4,6-trimethylisophthalic acid). Each contains either a macrometallocycle or a 1D zigzag chain as the subunit. The ligand-conformation and dimensionality control in these MOFs is discussed below.

Experimental Section

Materials and Physical Measurements. All chemicals used are as purchased without purification. Thermogravimetric experiments were performed using a TGA/SDTA851 instrument (heating rate of 10 °C/min, nitrogen stream).

Synthesis of 1. A mixture of $Ni(CH_3COO)_2\cdot 4H_2O$ (30 mg, 0.12 mmol), H_2TMIPA (20 mg, 0.12 mmol), and BITMB (10 mg, 0.03 mmol) was suspended in 15 mL mixed solvents of DMF, ethanol, and H_2O (v/v = 1:1:1), and heated in a Teflon-lined steel bomb at 100 °C for 4 days. A lot of green prism crystals formed were collected, washed with ethanol, and dried in the air. (Yield: 57%). Elemental anal.: Calcd for **1**: C, 57.85; H, 5.90; N, 9.64%. Found: C, 57.98; H, 5.78; N, 9.30%.

Synthesis of 2. A mixture of $Zn(NO_3)_2\cdot 6H_2O$ (30 mg, 0.11 mmol), H_2IPA (20 mg, 0.12 mmol), and BITMB (10 mg, 0.03 mmol) was suspended in 15 mL mixed solvents of DMF, ethanol, and H_2O (v/v = 1:1:1), and heated in a Teflon-lined steel bomb at 100 °C for 4 days. A lot of colorless stick crystals formed were collected, washed with ethanol, and dried in the air (yield: 44%). Elemental anal.: Calcd for **2**: C, 56.88; H, 4.96; N, 10.61%. Found: C, 56.45; H, 4.51; N, 10.42%.

Synthesis of 3. The similar procedure as prepared complex **2** except the mixed solvents of DMF and ethanol (v/v = 1:1) were used. The colorless prism crystals formed were collected, washed with ethanol, and dried in air. (Yield: 51%). Elemental anal.: Calcd for **3**: C, 57.86; H, 4.86; N, 10.80%. Found: C, 56.92; H, 4.56; N, 10.35%.

X-ray Structural Crystallography. Crystals of **1**−**3** mounted on glass fiber were studied with a Bruker SMART APEXII CCD Detector single-crystal X-ray diffractometer with a graphite-monochromated Mo−Kα radiation (λ = 0.71073 Å) source at 25 °C. All structures were solved by the direct method using the SHELXS program of the SHELXTL package and refined by the full-matrix least-squares method with SHELXL. The metal atoms in each complex were located from the E-maps, and other non-hydrogen atoms were located in successive difference Fourier syntheses and refined with anisotropic thermal parameters on F^2. The organic hydrogen atoms were generated geometrically (C−H 0.96 Å). The solvent molecules in **3** are highly disordered, and attempts to locate and refine were unsuccessful. The SQUEEZE program was used to remove scattering from the highly disordered solvent molecules and a new .HKL file was generated. The structure was solved by using the new generated .HKL file.

Results and Discussion

Syntheses. The assembly of an MOF is highly influenced by the ligand conformation and the coordination geometry of the metal ion.[14] In general, the ligand conformation can determine the structure of the final product. In our previous work, we focused our attention on the construction of novel metal−organic nanotubes based on 4,4′-bipyridine and benzenedicarboxylates. The metal ion was first connected by 4,4′-bipyridine to generate square or helical-chain subunits, which were further connected by the rigid carboxylate ligand to form 1D nanotubes.[11a,b] In this work, we substitute a flexible ligand, 1,3-bis(imidazol-1-ylmethyl)-2,4,6-trimethylbenzene (BITMB), in place of the rigid 4,4′-bipyridine for the structural subunit. The key properties of BITMB are (1) it is a strong bridging ligand that can link two metal ions; (2) it may possess two possible conformations, the *syn* and *anti* conformations (Scheme 1), which can connect metal ions to form subunits with varying topologies. It has been widely reported that the connection of metal ions by BITMB in the *syn* conformation will generate macrometallocycle or 1D zigzag chain subunits, while the connection of metal ions by BITMB in the *anti* conformation will form a 1D zigzag chain structure, as shown in Scheme 2. If these kinds of subunits are further connected by a secondary rigid carboxylate ligand, a MOF of higher dimensionality will be generated.

Scheme 1. The Two Conformations of BITMB

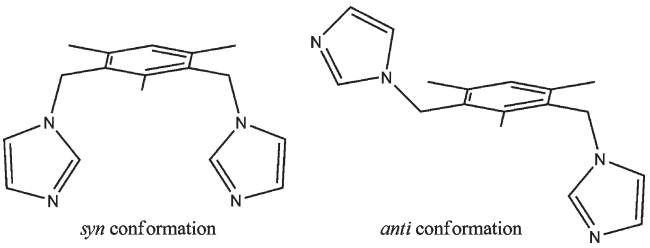

Scheme 2. The Possible Subunits Formed by BITMB with *syn*- or *anti*-Conformation

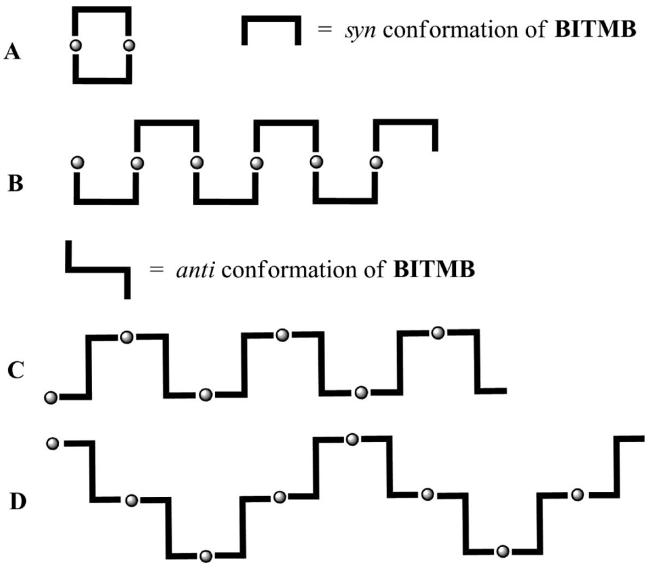

Considering these in mind, we constructed MOFs by reacting BITMB and a rigid benzenedicarboxylate with Ni(II) and Zn(II) ions. Three MOFs with macrometallocycles or 1D zigzag chains as building blocks containing BITMB in either the *syn* or *anti* conformation[15] have been solvothermally synthesized.

Crystal Structures. One-Dimensional Chain of Ni(BITMB)(TMIPA)·2H$_2$O (1). X-ray single crystal diffraction revealed that complex **1** has a 1D chain structure. The asymmetric unit consists of one nickel ion, one BITMB ligand, and one TMIPA ligand. As shown in Figure 1, the central nickel ion is coordinated by two nitrogen atoms from two BITMB ligands and four oxygen atoms from two chelating carboxylate groups of TMIPA, in which one oxygen atom of each carboxylate is only weakly coordinated with Ni−O distances of 2.162 and 2.189 Å. The average Ni−N and Ni−O distances are 2.028(7) and 2.117(5) Å, respectively. The metal environment is best described as a highly distorted octahedral geometry with one nitrogen [N(1A)] and one carboxylato-oxygen [O(2A)] occupying

Table 1. Crystal Data Collection and Structure Refinement for 1−3

	1	2	3
empirical formula	$C_{28}H_{30}N_4O_4Ni$	$C_{25}H_{24}N_4O_4Zn$	$C_{200}H_{196}N_{32}O_{34}Zn_8$
formula weight	545.27	509.85	4114.85
temp (K)	298(2)	273(2)	273(2)
crystal system	monoclinic	monoclinic	orthorhombic
space group	*Cc*	*C2/c*	*Pnma*
a (Å)	20.351(4)	26.179(5)	18.7077(11)
b (Å)	7.3805(16)	10.667(2)	24.8114(15)
c (Å)	18.116(4)	17.719(3)	21.5264(13)
α (deg)	90	90	90
β (deg)	98.893(4)	112.398(4)	90
γ (deg)	90	90	90
V (Å^3)	2688.3(10)	4574.8(14)	9991.8(10)
Z	4	8	2
*ρ*calc (g/cm^3)	1.347	1.481	1.368
F(000)	1144	2112	4264
data/restraints/params	4743 /2/ 334	5132 /0/307	11755/0/706
GOF on F^2	1.025	0.898	0.905
final *R* indices [$I > 2\sigma(I)$]	R1 = 0.0659, wR2 = 0.1586	R1 = 0.0701, wR2 = 0.1385	R1 = 0.0579, wR2 = 0.1615

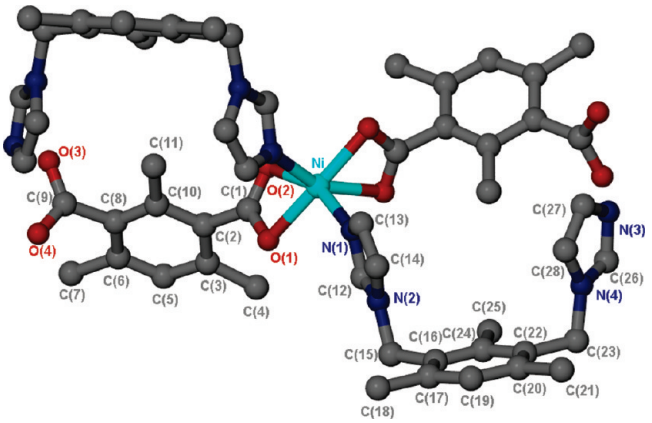

Figure 1. The coordination environment of the central nickel ion in **1**.

the axial positions, with the other nitrogen [N(1)] and oxygens [O(1), O(2), O(1A)] comprising the equatorial plane.

The BITMB ligand adopts the *syn* conformation, with both imidazole groups on the same side of the central benzene ring. The imidazole rings are almost perpendicular to the benzene ring, with an average dihedral angle of 90.45°. Both carboxylate groups of TMIPA remain deprotonated and chelate one nickel ion each. Because of the steric hindrance between the methyl groups and the carboxylate groups, the two carboxylate groups of TMIPA are not coplanar with the central benzene ring, with an average dihedral angle of 73.3°. Both BITMB and TMIPA adopt a bidentate coordination mode to connect two nickel ions. Thus, the nickel ions are infinitely connected by BITMB and TMIPA to generate a 1D chain (Scheme 2B) containing a 20-atom macrometallocycle formed by two nickel ions, one BITMB and one TMIPA ligand, with dimensions 3.9 × 9.1 Å. Each macrometallocycle is perpendicular to those adjacent, as shown in Figure 2. Hence, the 1D coordination chain can also be considered to be formed by repeating the macrometallocycles.

Two-Dimensional Interpenetrating Layer of Zn(BITMB)(IPA)·H$_2$O (2). Single crystal X-ray diffraction reveals that complex **2** crystallizes in the monoclinic space group *C*2/*c*. The asymmetric unit of **2** consists of one zinc ion, one BITMB, and one IPA ligand. The central zinc ion adopts a tetrahedral geometry and is coordinated by two oxygen

Table 2. The Selected Bond Lengths (Å) and Angles (deg) of Complexes 1−3

		1	
Ni−N1	2.023(7)	Ni−O1	2.063(5)
Ni−N3	2.032(6)	Ni−O2	2.162(5)
Ni−O4	2.055(5)	Ni−O3	2.189(5)
N1−Ni−N3	95.6(3)	N3−Ni−O4	93.9(2)
N1−Ni−O4	97.4(2)	N1−Ni−O1	94.7(2)
O4−Ni−O1	163.6(2)	N3−Ni−O1	95.8(2)
N1−Ni−O2	157.2(2)	N3−Ni−O2	90.0(2)
O4−Ni−O2	104.2(2)	O1−Ni−O2	62.7(2)
N1−Ni−O3	89.0(2)	N3−Ni−O3	155.7(2)
O4−Ni−O3	61.8(2)	O1−Ni−O3	107.6(2)
O2−Ni−O3	94.8(2)		
		2	
Zn−O1	1.974(4)	Zn−N3	2.015(5)
Zn−O3	1.985(4)	Zn−N1	2.015(5)
O1−Zn−O3	100.18(18)	O3−Zn−N1	97.75(19)
O1−Zn−N1	115.22(18)	O1−Zn−N3	106.84(19)
O3−Zn−N3	123.7(2)	N1−Zn−N3	112.9(2)
		3	
Zn2−N1	2.018(4)	Zn2−O7	2.025(4)
Zn2−O3	2.038(4)	Zn1−O5	2.017(4)
Zn1−O1	1.993(4)	Zn1−N7	2.011(4)
Zn3−O9	1.950(3)	Zn3−O12	1.940(3
Zn3−N5	2.018(4)	Zn3−N3	1.991(4)
N1−Zn2−N1	130.9(2)	N1−Zn2−O7	99.19(11)
N1−Zn2−O7	99.19(11)	N1−Zn2−O3	109.19(10)
N1−Zn2−O3	109.19(10)	O7−Zn2−O3	105.10(16)
O1−Zn1−N7	105.36(12)	N7−Zn1−N7	111.7(2)
O1−Zn1−O5	104.46(17)	N7−Zn1−O5	114.42(11)
N7−Zn1−O5	114.42(11)	O12−Zn3−O9	108.88(14)
O12−Zn3−N3	123.42(15)	O9−Zn3−N3	104.59(14)
O12−Zn3−N5	102.90(14)	O9−Zn3−N5	97.28(14)
N3−Zn3−N5	116.59(15)		

atoms from different IPA ligands and two nitrogen atoms from different BITMB ligands. The Zn−O and Zn−N distances range from 1.974 to 2.015 Å. As in **1**, the BITMB adopts the *syn* conformation, with the two imidazole rings on the same side of the benzene ring; in this conformation the BITMB ligand connects two zinc ions. The average dihedral angle between the central benzene ring and the two imidazole rings is 91.3°, which is slightly larger than that in **1**. Unlike in **1**, the IPA ligand is nearly planar, with a dihedral angle of 8.75° between carboxylate groups and the benzene ring.

In contrast with **1**, in which the BITMB and TMIPA ligands connect nickel ions to form a 20-membered macrometallocycle, in complex **2**, two BITMB ligands link two

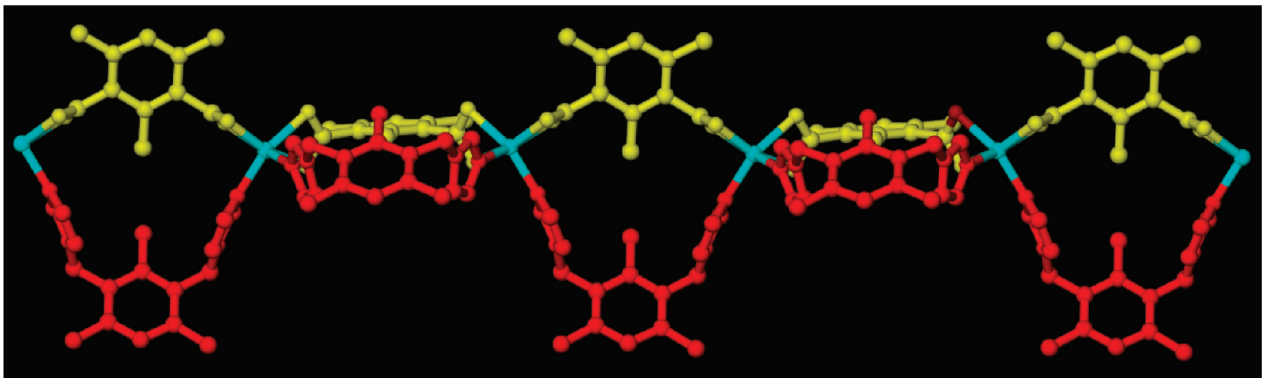

Figure 2. The 1D coordination chain of **1**, with BITMB shown in red and TMIPA in yellow.

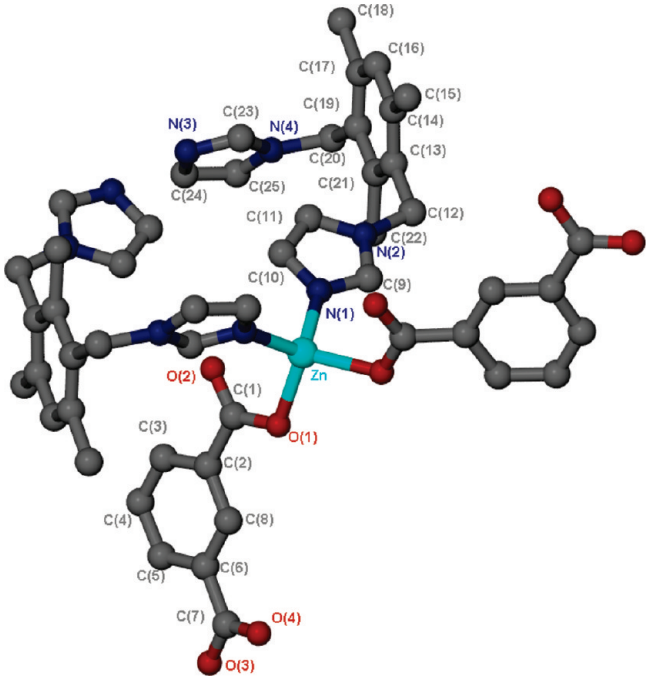

Figure 3. The coordination environment of the central zinc ion in **2**.

zinc ions to generate a 24-membered macrometallocycle with dimensions 3.6 × 12.6 Å (Scheme 2A and Supporting Information). The macrometallocycles can be considered subunits of the whole structure. Both carboxylate groups of IPA are deprotonated during the reaction and the ligand adopts a bidentate bridging mode to link two zinc ions. Thus, every IPA ligand connects two macrometallocycle subunits and each macrometallocycle subunit attaches to four IPA ligands to result in the formation of a 2D layer containing rectangular windows of dimension 7.1 × 17.0 Å (Figure 4a). If the macrometallocycle subunit is considered a single node and the IPA ligand a linear linker, then the layer possesses a (4,4) net,[16] as shown in Figure 4b.

Because of the large windows in the 2D layer, it is not surprising that interweaving results. Two 2D layers interweave to form a 2D interpenetrating framework, as shown in Figure 4c. The macrometallocycle subunit in one layer is positioned at the center of the rectangular window of a second layer (Figure 4d). Figure 5 shows the 3D packing of complex **2**.

Three-Dimensional Porous Framework of Zn_2(BITMB)$_2$-(HIPA)$_2$(IPA)·H_2O (3). Single crystal X-ray diffraction reveals that complex **3** crystallizes in the orthorhombic space group *Pnma* and has a 3D porous framework based on 1D Zn-BITMB chains. Figure 6 shows the coordination environment of the zinc ions in **3**. The asymmetric unit of **3** consists of one zinc ion and half each of two additional zinc ions, three IPA ligands, two BITMB ligands and one uncoordinated water molecule. Each zinc ion (Zn1, Zn2, and Zn3) adopts a tetrahedral geometry and is coordinated by one nitrogen atom each from two BITMB ligands one oxygen atom each from two IPA ligands. The Zn−N and Zn−O distances range from 1.991(4) to 2.018(4) Å and 1.940(3) to 2.038(4) Å, respectively.

Because of the similar coodination environment of three zinc ions, each zinc ion can be considered as a single node and the IPA ligands and the BITMB ligands as linear bridging linkers, and then the structure possesses a diamond-type network,[17] as shown in Figure 7.

Unlike that found in complexes **1**−**2**, the BITMB ligand in **3** adopts the *anti* conformation, with the two imidazole rings on opposite sides of the central benzene ring. The average dihedral angle between the benzene ring and the imidazole rings is 95.4°, which is slightly larger than those in complexes **1**−**2**. Thus, Zn1, Zn2, and Zn3 ions are connected by BITMB ligands to form two similar 1D zigzag chains (Figure 8a: A and B, Scheme 2: D) with the nearest Zn···Zn distance 11.55 Å between two chains. The zigzag chains run in opposite directions along the *b* axis. These chains are further connected by the IPA ligands through monodentate carboxylate groups coordinating to Zn1 and Zn2, resulting in the formation of a 2D layer (Figure 8b) with the nearest Zn···Zn distance 8.392 Å between two chains. The A and B chains alternate within the layer. To the best of our knowledge, the connection of metal ions by a bridging BITMB ligand in the *anti* conformation normally generates a 1D zigzag chain as shown in Scheme 2 (type C). The 1D zigzag chain (Scheme 2 type D) as found in **3** is heretofore unreported in the study of BITMB and its derivatives.

It should be pointed out that the *anti* conformation of BITMB ligand exists as a pair of enantiomers, which alternate within the 1D zigzag chain (Figure 8c). The 1D Zn-IPA chain generated by IPA connecting Zn1 and Zn2 ions is located on the crystallographic mirror plane between the two enantiomers. The 2D layers are further connected by IPA ligands through the monodentate carboxylate group coordinating to Zn3 ions to complete the tetrahedral geometry of Zn3, providing a 3D porous framework along the *a* axis (Figure 9). The dimensions of the channels are 5.0 × 6.5 Å (from atom to atom) with 9.3% solvent-accessible volume

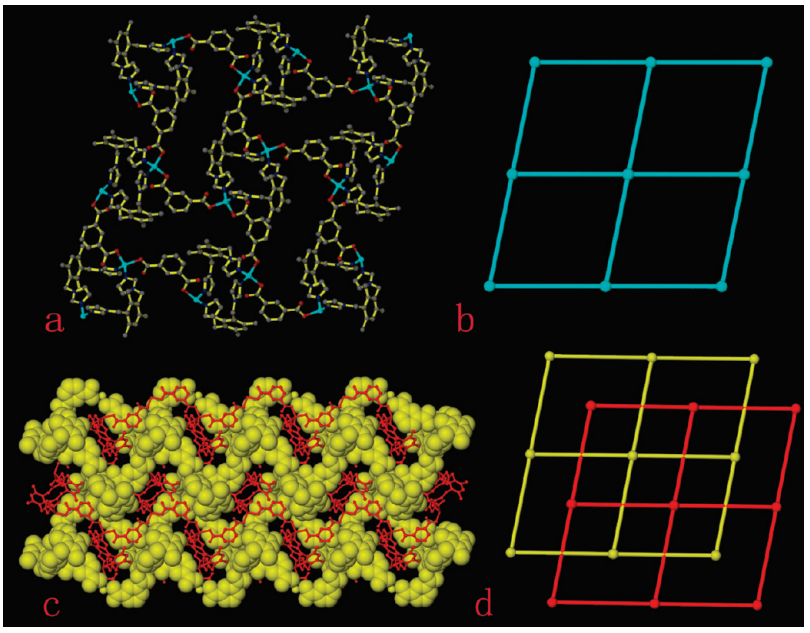

Figure 4. (a) The 2D layer; (b) the (4,4) net of **2**; (c) the interpenetrating layer shown in space-filling and ball-and-stick representations; and (d) schematic representation of the interpenetrating layer.

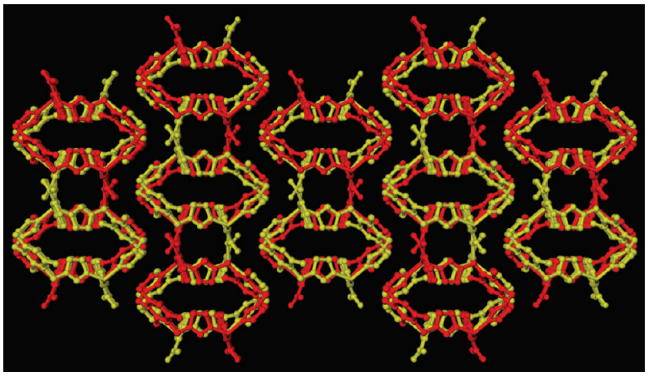

Figure 5. The 3D packing of **2** along the *c* axis. The interpenetrating layers are shown in different colors.

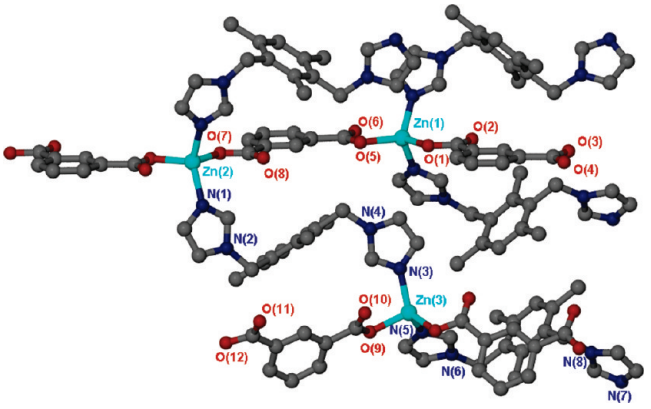

Figure 6. The coordination environment of zinc ions in **3**.

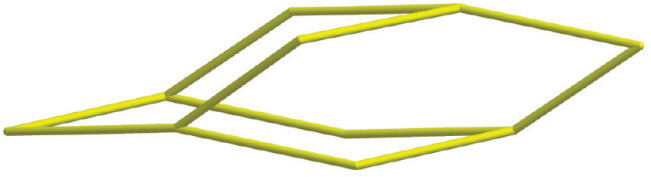

Figure 7. A single diamond-type network in **3**.

calculated from PLATON, in which the uncoordinated water molecules reside.

In the 3D framework, two different Zn-IPA chains exist, as shown in Figure 10. One is generated by IPA connecting Zn1 and Zn2 ions (Zn1,2-IPA chain), and the other is generated by IPA connecting Zn3 ions (Zn3-IPA chain). The two chains are quite different and play different roles in the formation of the final porous framework. All IPA ligands in the 1D Zn1,2-IPA chain are planar, and connect the 1D Zn-BITMB chains to form the 2D layer, while the IPA ligands in the 1D Zn3-IPA chain are not planar, with an average dihedral angle of 58.0°, and connect the 2D layer to generate the final 3D porous framework.

Thermal Stabilities of 1−3. Thermogravimetric analysis (TGA) was performed on complexes **1**−**3**. A TGA study on an as-isolated crystalline sample of **1** shows a 5.9% weight loss from 105 to 137 °C, corresponding to the loss of two uncoordinated water molecules (calcd: 6.1%). There is no weight loss from 137 to 370 °C. After 370 °C, **1** starts to decompose. For complex **2**, the gradual weight loss of 3.1% from 50 to 240 °C is equal to the loss of one uncoordinated water molecule (calcd: 3.4%). There is no further loss from 250 to 400 °C, and after that temperature, **2** starts to decompose. For complex **3**, from 50 to 200 °C, there is a weight loss of 1.4%, which corresponds to the loss of one uncoordinated water molecule (calcd: 1.4%). There is no weight loss until 330 °C, at which complex **3** starts to decompose. All three complexes decompose sharply after about 445 °C due to the degradation of the organic ligands.

Photoluminescence Properties of 2 and 3. Photoluminescence measurements at room temperature of **2** and **3** in the solid state show that both coordination networks exhibit similar, strong luminescence at λ_{max} = 460, 548, and 676 nm, respectively, upon excitation at 250 nm (Figure 11), which can be assigned to an intraligand $\pi \rightarrow \pi^*$ transition.[18] These

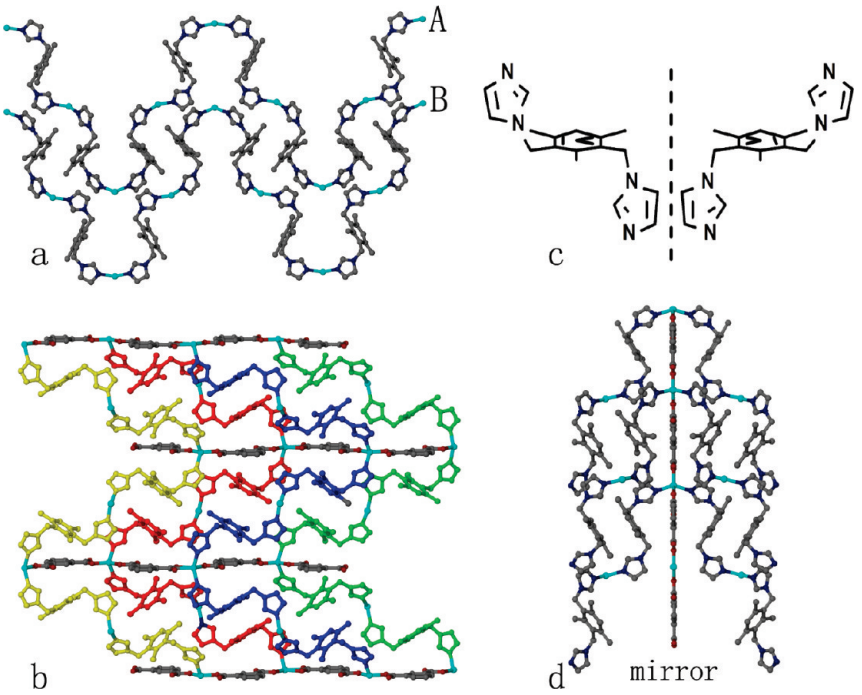

Figure 8. (a) The 1D zigzag chain; (b) the 2D layer; (c) the enantiomers of the *anti* conformational BITMB; and (d) the 1D Zn-IPA chain acting as the mirror of the enantiomers of the *anti* conformational BITMB.

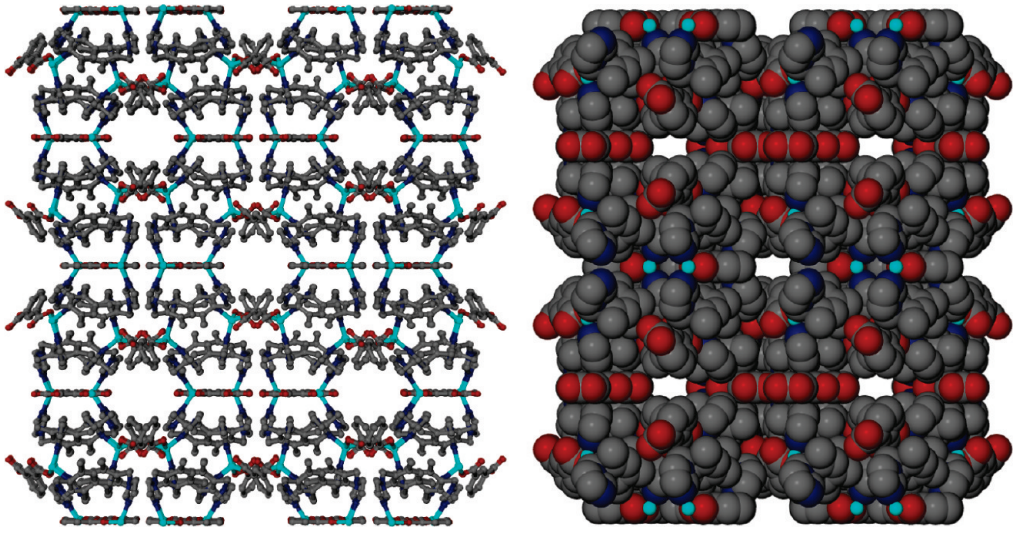

Figure 9. The 3D porous framework of **3** in ball-and-stick (left) and space-filling (right) representations.

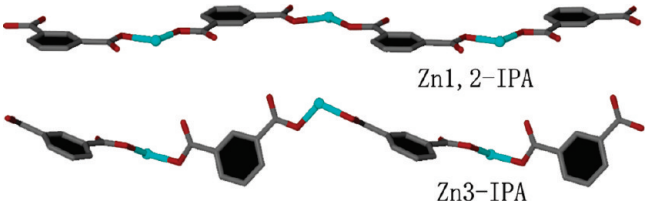

Figure 10. The different arrangements of the two Zn-IPA chains.

observations suggest that the coordination of the BITMB and IPA ligands with Zn^{2+} ions has no influence on the emission mechanism of the metal−organic coordination polymers,[19] although increasing the intensity of intraligand fluorescent emission due to the coordination of BITMB and

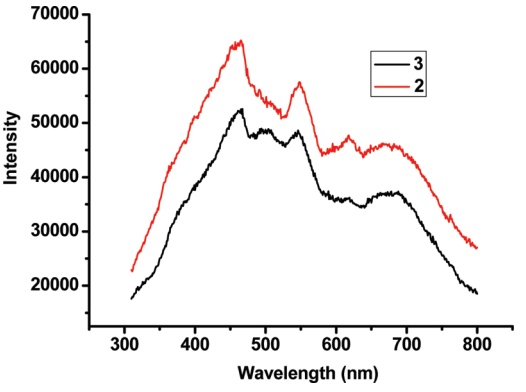

Figure 11. Solid-state emission spectra of **2** and **3**.

Scheme 3. Solvent-Induced Conformation and Dimensionality Control in 2 and 3

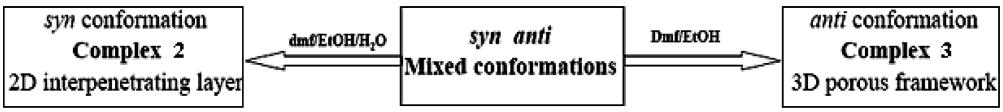

Scheme 4. Schematic Representation of the Control of Ligand Conformation and Dimensionality in Complexes 1−3

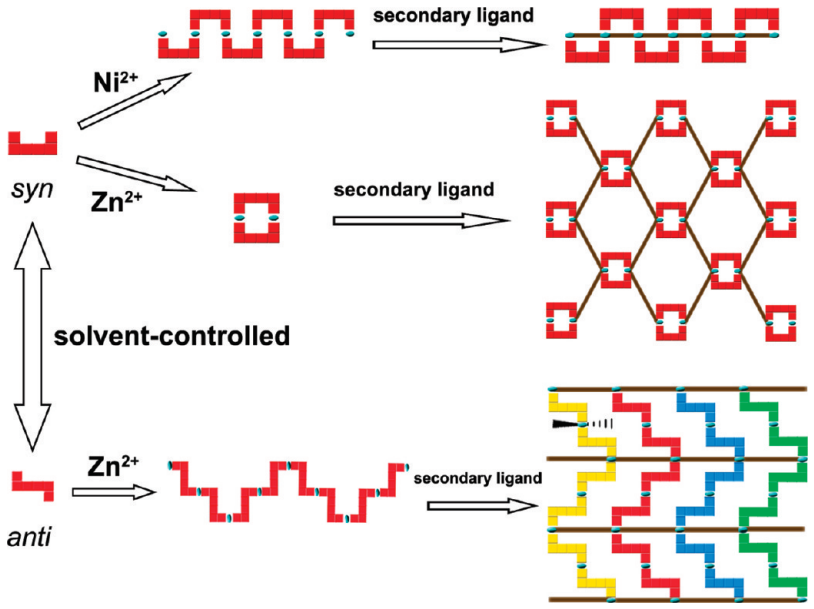

IPA ligands to the metal ion, thereby increasing the rigidity of the ligand and reducing the nonradiative decay of the intraligand excited state.[20]

Effect of Solvents on the Structures of 2 and 3. It is well-known that the solvent can have a significant structure-directing effect on the formation of MOFs.[21] The same reaction in different solvents may result in different structural topologies. The ratio of reagents, the reaction temperature, and time are the same for the syntheses of complexes **2** and **3**, differing only in solvents used. As described above, complexes **2** and **3** have quite different structures: complex **2** is a 2D interpenetrating layer based on a Zn-BITMB macrometallocycle, while complex **3** is a 3D porous framework based on 1D Zn-BITMB zigzag chains. The structural difference between complexes **2** and **3** results from the different solvents used in the synthesis. **2** was synthesized using DMF, EtOH, and H_2O (v/v = 1:1:1) as the solvents, while **3** was obtained without the presence of water in the reaction system, which indicates that water plays an important role in the formation of the different structures of **2** and **3**. More interestingly, the BITMB ligand adopts different conformations in **2** and **3**, as shown in Scheme 3. Recently, a few reports concerning the conformational control of a flexible ligand have been documented; however, examples such as **2** and **3**, in which the addition of water to the reaction mixture not only controls the conformation of BITMB ligand, but also alters the dimensionalities of the complexes, are quite rare.

Effects of Ligand Conformation on Structures of 1−3. The assembly of metal ions and ligands into MOFs can be regarded as a programmed system in which the stereo- and reactivity information stored in the ligands is read by the metal ions through an algorithm defined by their coordination geometry.[22] The ligand conformation can determine the structural topology of the final product, which should always be taken into account in the design and synthesis of MOF with desired topologies. In our work, the BITMB ligand can possess *syn* or *anti* conformations, as shown in Scheme 1. The two conformations of BITMB may result in MOFs with different structural topologies. In complexes **1** and **2**, the BITMB adopts the *syn* conformation to connect the metal ions to generate a macrometallocycle (complexes **2**) or chain (complex **1**) as the subunits; in **3**, the BITMB ligand adopts the *anti* conformation, connect zinc ions to form a 1D zigzag chain as the subunit. However, the 1D zigzag chains in complexes **1** and **3** are quite different, as shown in Scheme 2B,D. Furthermore, the rigid TMIPA in **1** is nonplanar, allowing it to chelate the nickel ion through its two carboxylate groups to further stabilize the 1D chain. However, the IPA ligand in **3** is planar, and both carboxylate groups of IPA adopt a monodentate coordination mode to connect one zinc ion each, resulting in the formation of a 3D porous framework, which provides further evidence that the planarity of the ligand has a significant effect on the structure of the final product. In complexes **2**, the BITMB ligands in the *syn* conformation connect zinc ions to generate a 24-membered ring as the subunit, which is further connected by the monodentate IPA along the *bc* plane to give rise to the 2D (4,4) net. Hence, the BITMB ligand in the *syn* conformation gives rise to frameworks of low dimensionality, while the *anti* conformation of BITMB can generate higher-dimensional frameworks, when used in a mixed-ligand synthesis to construct a MOF. The conformation of BITMB can be controlled by the presence water in the reaction mixture, and the conformation of the BITMB further controls the dimensionality of the final product (Scheme 4).

Conclusions

In conclusion, three MOFs based on flexible BITMB and rigid benzenedicarboxylates have been synthesized and characterized. The flexible BITMB adopts *syn* or *anti* conformations in the complexes, which can be controlled by the presence or lack of water in the reaction. More interestingly, the dimensionality of the product can be controlled by the ligand conformation of BITMB. To the best of our knowledge, this is the first example (complexes **2** and **3**) that the conformation of the ligand and the dimensionality of the product can be concurrently controlled by the solvent in the reaction system. Current work further indicates that the ligand conformation has a significant effect on the structure of the final product, and by controlling the conformation of the flexible ligand, various MOFs with different structural topologies can be constructed.

Acknowledgment. This work was supported by the National Natural Science Foundation of China (Grant 20701025), the Natural Science Foundation of Shandong Province (Y2008B01), and Shandong University.

Supporting Information Available: Three X-ray crystallographic files in CIF format and TGA curve for complexes **1**−**3**. These materials are available free of charge via the Internet at http://pubs.acs.org.

References

(1) For reviews, see (a) Eddaoudi, M.; Moler, D. B.; Li, H. L.; Chen, B. L.; Reineke, T. M.; O'Keeffe, M.; Yaghi, O. M. *Acc. Chem. Res.* **2001**, *34*, 319. (b) Janiak, C. *Dalton Trans.* **2003**, 2781. (c) Ferey, G.; Mellot-Draznieks, C.; Serre, C.; Millange, F. *Acc. Chem. Res.* **2005**, *38*, 217. (d) Bradshaw, D.; Claridge, J. B.; Cussen, E. J.; Prior, T. J.; Rosseinsky, M. J. *Acc. Chem. Res.* **2005**, *38*, 273. (e) Kitagawa, S.; Kitaura, R.; Noro, S. *Angew. Chem., Int. Ed.* **2004**, *43*, 2334.

(2) (a) Wang, Z. Q.; Kravtsov, V. C.; Zaworotko, M. J. *Angew. Chem., Int. Ed.* **2005**, *44*, 2877. (b) Prior, T. J.; Bradshaw, D.; Teat, S. J.; Rosseinsky, M. J. *Chem. Commun.* **2003**, 500. (c) Dybtsev, D. N.; Nuzhdin, A. L.; Chun, H.; Bryliakov, K. P.; Talsi, E. P.; Fedin, V. P.; Kim, K. *Angew. Chem., Int. Ed.* **2006**, *45*, 916. (d) Pan, L.; Olson, D. H.; Ciemnolonski, L. R.; Heddy, R.; Li, J. *Angew. Chem., Int. Ed.* **2006**, *45*, 616.

(3) (a) Pan, L.; Sander, M. B.; Huang, X.; Li, J.; Smith, M. R., Jr.; Bittner, E. W.; Bockrath, B. C.; Johnson, J. K. *J. Am. Chem. Soc.* **2004**, *126*, 1308. (b) Foster, P. M.; Kim, D. S.; Cheetham, A. K. *Solid State Sci.* **2005**, *7*, 594. (c) Férey, G.; Mellot-Draznieks, C.; Serre, C.; Millange, F.; Dutour, J.; Surblé, S.; Margiolaki, I. *Science* **2005**, *309*, 2040. (d) Ko, J. W.; Min, K. S.; Suh, M. P. *Inorg. Chem.* **2002**, *41*, 2151.

(4) (a) Ferey, G. *Chem. Mater.* **2001**, *13*, 3084. (b) Rao, C. N. R.; Natarajan, S.; Vaidhyanathan, R. *Angew. Chem., Int. Ed.* **2004**, *43*, 1466. (c) Zaworotko, M. J. *Angew. Chem., Int. Ed.* **2000**, *39*, 3052.

(5) (a) Narinho, M. V.; Yoshida, M. I.; Guedes, K. J.; Krambrock, K.; Bortoluzzi, A. J.; Hörner, M.; Machado, F. C.; Teles, W. M. *Inorg. Chem.* **2004**, *43*, 1539. (b) Zhang, X.; Guo, G. C.; Zheng, F. K.; Zhou, G. W.; Mao, J. G.; Dong, Z. C.; Huang, J. S.; Mak, T. C. W. *J. Chem. Soc., Dalton Trans.* **2002**, 1344.

(6) (a) Su, C. Y.; Cai, Y. P.; Chen, C. L.; Smith, M. D.; Kaim, W.; Loye, H. C. *J. Am. Chem. Soc.* **2003**, *125*, 8595. (b) Liu, H. K.; Sun, W. Y.; Ma, D. J.; Yu, K. B.; Tang, W. X. *Chem. Commun.* **2000**, 591.

(7) (a) Zhang, J.; Chew, E.; Chen, S. M.; Pham, J. T. H.; Bu, X. H. *Inorg. Chem.* **2008**, *47*, 3495. (b) Wang, X. T.; Wang, X. H.; Wang, Z. M.; Gao, S. *Inorg. Chem.* **2009**, *48*, 1301. (c) Peng, R.; Li, D.; Wu, T.; Zhou, X. P.; Ng, S. W. *Inorg. Chem.* **2006**, *45*, 4035. (d) Dong, Y. B.; Jiang, Y. Y.; Li, J.; Ma, J. P.; Liu, F. L.; Tang, B.; Huang, R. Q.; Batten, S. R. *J. Am. Chem. Soc.* **2007**, *129*, 4520.

(8) (a) Yang, X. D.; Ranford, J. D.; Vittal, J. J. *Cryst. Growth Des.* **2004**, *4*, 781. (b) Ding, B.; Liu, Y. Y.; Huang, Y. Q.; Shi, W.; Cheng, P.; Liao, D. Z.; Yan, S. P. *Cryst. Growth Des.* **2009**, *9*, 593. (c) Shi, Z.; Zhang, L. R.; Gao, S.; Yang, G. Y.; Hua, J.; Gao, L.; Feng, S. H. *Inorg. Chem.* **2000**, *39*, 1990. (d) Hirsch, K. A.; Wilson, S. R.; Moore, J. S. *Inorg. Chem.* **1997**, *36*, 2960.

(9) (a) Wan, S. Y.; Li, Y. Z.; Okamura, T.; Fan, J.; Sun, W. Y.; Ueyama, N. *Eur. J. Inorg. Chem.* **2003**, 3783–3789. (b) hang, Z. H.; Shen, Z. L.; Okamura, T.; Zhu, H. F.; Sun, W. Y.; Ueyama, N. *Cryst. Growth Des.* **2005**, *5*, 1191–1197. (c) Liu, G. X; Huang, Y. Q.; Chu, Q.; Okamura, T.; Sun, W. Y.; Liang, H.; Ueyama, N. *Cryst. Growth Des.* **2008**, *8*, 3233–3245. (d) Zhang, Z. H.; Okamura, T.; Hasegawa, Y.; Kawaguchi, H.; Kong, L. Y. *Inorg. Chem.* **2005**, *44*, 6219–6227. (e) Zhu, H. F.; Fan, J.; Okamura, T.; Zhang, Z. H.; Liu, G. X.; Yu, K. B. *Inorg. Chem.* **2006**, *45*, 3941–3948.

(10) (a) Jin, H.; Qi, Y. F.; Wang, E. B.; Li, Y. G.; Wang, X. L.; Qin, C.; Chang, S. *Cryst. Growth Des.* **2006**, *6*, 2693. (b) Li, X. J.; Cao, R.; Sun, D. F.; Bi, W. H.; Wang, Y. Q.; Li, X.; Hong, M. C. *Cryst. Growth Des.* **2004**, *4*, 775. (c) Xue, M.; Zhu, G. S.; Ding, H.; Wu, L.; Zhao, X. J.; Jin, Z.; Qiu, S. L. *Cryst. Growth Des.* **2009**, *9*, 1481.

(11) (a) Dai, F. N.; He, H. Y.; Sun, D. F. *J. Am. Chem. Soc.* **2008**, *130*, 14064. (b) Dai, F. N.; He, H. Y.; Sun, D. F. *Inorg. Chem.* **2009**, *48*, 4613. (c) He, H. Y.; Dai, F. N.; Xie, A. P.; Tong, X.; Sun, D. F. *CrystEngComm* **2008**, *10*, 1429.

(12) (a) Su, C. Y.; Cai, Y. P.; Chen, C. L.; Smith, M. D.; Kaim, W.; zur Loye, H. −C. *J. Am. Chem. Soc.* **2003**, *125*, 8595. (b) Liu, J.; Liu, H. K.; Feng, X. L.; Zhang, H. X.; Zhou, Z. Y.; Chan, A. S. C.; Kang, B. S. *Inorg. Chem. Commun.* **2001**, *4*, 674. (c) Wang, X. F.; Lv, Y.; Okamura, T.; Kawaguchi, H.; Wu, G.; Sun, W. Y.; Ueyama, N. *Cryst. Growth Des.* **2007**, *7*, 1125.

(13) Bi, W. H.; Cao, R.; Sun, D. F.; Yuan, D. Q.; Li, X.; Wang, Y. Q.; Li, X. J.; Hong, M. C. *Chem. Commun.* **2004**, 2104.

(14) Sun, D. F.; Collins, D. J.; Ke, Y. X.; Zhou, H. C. *Chem.—Eur. J.* **2006**, *12*, 3768.

(15) (a) Kumar, D. K.; Das, A.; Dastidar, P. *Cryst. Growth Des.* **2007**, *7*, 205. (b) Zhang, L.; Lu, X. Q.; Chen, C. L.; Tan, H. Y.; Zhang, H. X.; Kang, B. S. *Cryst. Growth Des.* **2005**, *5*, 283.

(16) Kumar, D. K.; Jose, D. A.; Das, A.; Dastidar, P. *Inorg. Chem.* **2005**, *44*, 6933.

(17) (a) Lin, H. S.; Maggard, P. A. *Inorg. Chem.* **2009**, *48*, 8940. (b) Wang, Z. M.; Zhang, B.; Kurmoo, M.; Green, M. A.; Fujiwara, H.; Otsuka, T.; Kobayashi, H. *Inorg. Chem.* **2005**, *44*, 1230.

(18) Wang, S. T.; Hou, Y.; Wang, E. B.; Li, Y. G.; Xu, L.; Peng, J.; Liu, S. X.; Hu, C. W. *New J. Chem.* **2003**, *27*, 1144.

(19) Clares, M. P.; Aguilar, J.; Aucejo, R.; Lodeiro, C.; Albelda, M. T.; Pina, F. J.; Lima, C.; Parola, A. J.; Pina, J.; De Melo, J. S.; Soriano, C.; García-España, E. *Inorg. Chem.* **2004**, *43*, 6114.

(20) Zheng, C. G.; Xie, Y. L.; Xiong, R. G.; You, X. Z. *Inorg. Chem. Commun.* **2001**, *4*, 405.

(21) (a) Delhaye, L.; Ceccato, A.; Jacobs, P.; Kottgen, C.; Merschaert, A. *Org. Proc. Res. Dev.* **2007**, *11*, 160. (b) Kadish, K. M.; Wang, L. L.; Thuriere, A.; Giribabu, L.; Garcia, R.; Caemelbecke, E. V.; Bear, J. L. *Inorg. Chem.* **2003**, *42*, 8309.

(22) (a) Lehn, J. M. *Supramolecular Chemistry − Concepts and Perspectives*; VCH: Weinheim, 1995. (b) Hong, M. C.; Su, W. P.; Cao, R.; Fujita, M.; Lu, J. X. *Chem.—Eur. J.* **2000**, *6*, 427. (c) Cao, R.; Sun, D. F.; Liang, Y. C.; Hong, M. C.; Tatsumi, K.; Shi, Q. *Inorg. Chem.* **2002**, *41*, 2087.